Hybrid Coacervate-in-Liposome Systems

F. S. Brandenburg

Technische Universiteit Delft

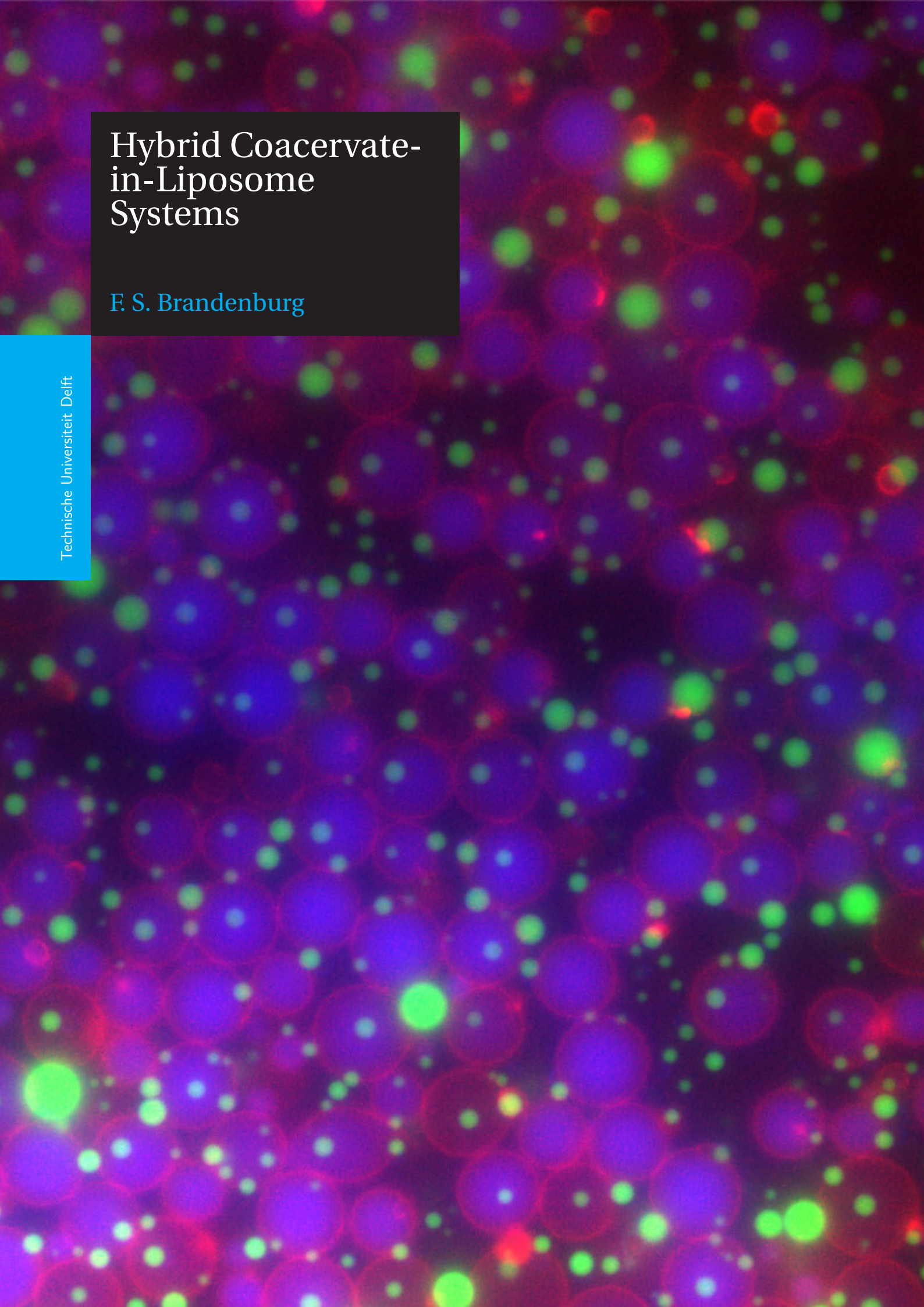

HYBRID COACERVATE-IN-LIPOSOME SYSTEMS

by

F. S. Brandenburg

in partial fulfillment of the requirements for the degree of

Bachelor of Science
in Applied Physics

at the Delft University of Technology,
to be defended publicly on Tuesday August 7, 2018 at 16:00 AM.

Supervisor:	Prof. dr. Cees Dekker	
Thesis committee:	Dr. Siddarth R. Deshpande,	TU Delft
	Dr. Chirlmin Joo,	TU Delft

An electronic version of this thesis is available at http://repository.tudelft.nl/.

ACKNOWLEDGEMENTS

Firstly I would like to thank professor Cees Dekker whose captivating honours course sparked the first interest in doing a project at his lab. I also want to thank Siddarth Deshpande whose enthusiastic demeanour and careful guidance has helped me tremendously during this project. I'm Sreekar Wunnava also very thankful for his help in the lab. His willingness to set aside his own work and take time to help me has proven invaluable and shows his good character. Next I would like to thank Jacob Kerssemakers and Louis Reese for their advice in analysing the data. I would like to thank Kevin Charles, Jaco van der Torre, Anthony Birnie, Stein Faes and Mart Last for other general help in the lab and debugging of problems. Lastly I would like to thank all other Cees Dekker lab members who made my time here as pleasant as possible.

F. S. Brandenburg
Delft, August 2018

Contents

1

INTRODUCTION

1.1. SYNTHETIC CELLS

If one looks around in nature one may overwhelmed by the diversity and complexity of living organisms. A valid idea would then be to look inside, and look at the inner workings of these organism. However one is likely to find an equally, if not more, complex system of vessels, organs, neurons and other subsystems. A good scientist may then say: "Let's look at the most essential motif of living organisms, of which everything is made, let's look at the cell!" If one might think he has now arrived at simple building blocks with which he can build his understanding of the larger whole will likely be sorely disappointed, because the cell level might be the most complex of all. After eons of evolution nature has come up with an system that certainly works, but there is no evolutionary pressure for it to be elegant or minimalist or easy to understand. One approach to combat is to go bottom-up and to try and reduce this complexity by designing a synthetic cell only comprised of the most essential parts, a minimal cell. A minimal cell should only include the most essential functions such as metabolism and replication. In the ideal case such a cell would resemble the proto-cell from which all life has spawn, and may therefore gift us with answers about some of the most quintessential questions of mankind: the origin of life itself.

1.2. LIPOSOMES

In our quest of building this minimal cell it should come naturally to start with the very thing that separates the cell from it's environment, which is of the cell membrane. In nature these cell membranes are made from phospholipid bilayers. Phospholipids are molecules that are composed of a hydrophillic head and hydrophobic tail (see figure 1.1).

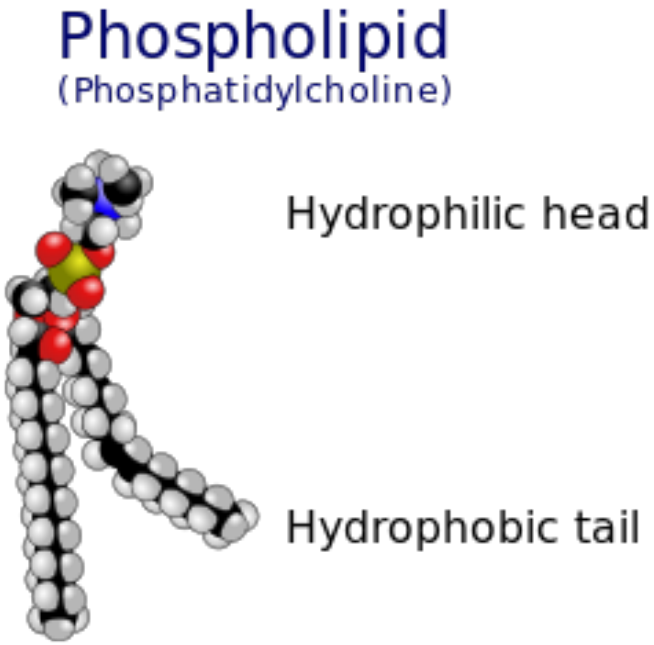

Figure 1.1: A phospholipid has a hydrophillic head and a hydrophobic tail [1]. This particular phospholipid called DOPC was used to conduct all experiments in this thesis.

Hydrophillic components are attracted to polar environments such as water while hydrophobic components are repulsed by it. Phospholipids freely floating in solution are therefore not energetically favourable. To minimise their energy, they self-assemble into a supra-molecular structures[2]. A few of these structures are: bilayers, micelles and liposomes. These structures are shown in figure 1.2.[3][4]

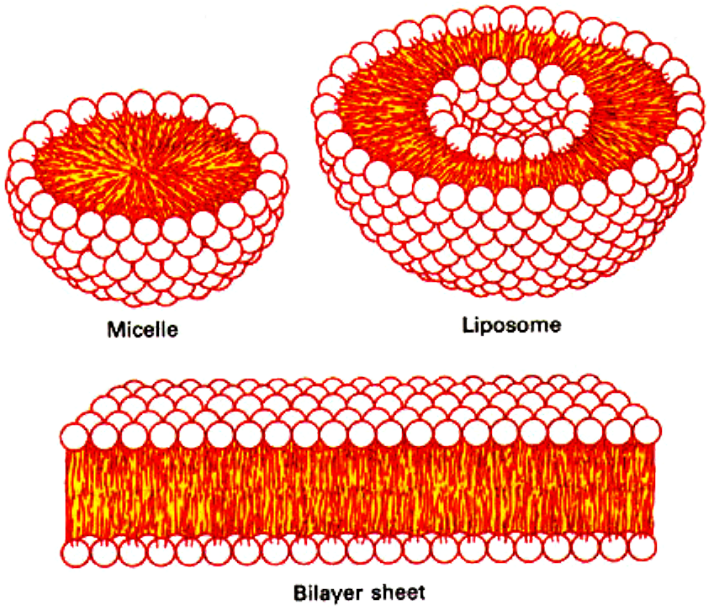

Figure 1.2: A few phospholipid assemblies including the micelle, the liposome and the bi-layer [5].

Of these structures the bilayer has the lowest bending energy since it has zero curvature. However because it's open ends are energetically unfavourable the phospholipids would rather form a spherical bi-layer called a liposome. Depending on the specific conditions, micelles could also be formed.

Liposomes are a good candidate for our synthetic membrane because they are very similar to the cell membrane of existing organisms.

1.3. COACERVATES

Another way to separate the interior from the exterior is strangely enough without any physical membrane but by forming coacervates. Coacervates are liquid-liquid phase separations that arise spontaneously. Normally the laws of thermodynamics tell us that systems will always go to higher entropy (more disordered) states. However because coacervates are energetically favourable it possible for this subsystem to go the other way around: from disorder (molecules uniformly dispersed across the solution) it will go to an ordered state , (almost) all molecules are in one spot. However the entropy of the the entire system still increases. Coacervates play a central role in Alexander Oparin's "primordial soup" hypothesis for the origin of life. In this theory he proposes that life could have originated in coacervates of polyaminoacids in the Archaic water pools of the young Earth. The replicating DNA formed a secondary coacervate (coacervates in coacervates), giving the origin to the first eukaryotic cells. [6]

The basic process behind coacervation is that it's components have a higher affinity with each other then with the rest of the solution.[7] There are two types of coacervation: simple and complex. Simple coacervation can occur by changing the solvent conditions. A molecule can then form coacervates with high concentrations of the molecule and one of the solvents. The dilute phase will consists mainly of the other solvent. The molecule can move between phases and will enter an equilibrium. Complex coacervation occurs when two different different polymers are attracted to each other. This can be on the basis of electrostatic forces, van der Waals forces, hydrophillic attraction or mechanisms. [8]. These polymers will then spontaneously demix from the solute. The coacervates we will use are complex coacervates based on the electrostatic forces. These long positively or negatively charged polymers can overcome the entropic barrier and spontaneously clump together. [9] [10]. [11]

Coacervates are also ubiquitous in the cellular world. For example P-granules and nucleoi could be seen as examples of coacervates in cells.[12] [13] And these coacervates bring advantages with them. A coacervate for example has a much higher concentration then its surroundings which of course makes it possible for certain reactions to happen faster or more easily. [7]

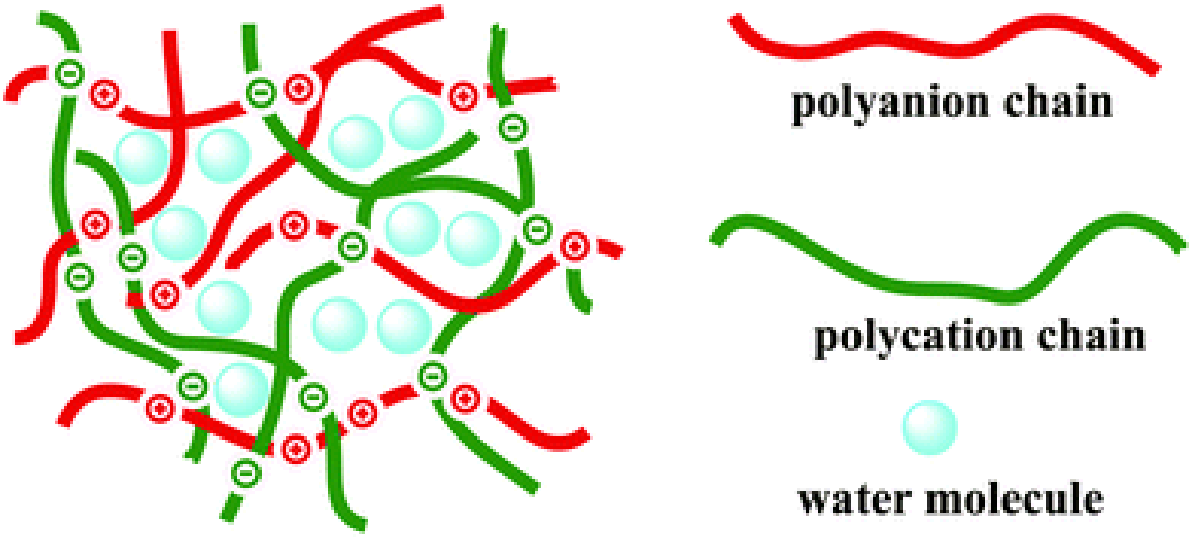

Figure 1.3: Schematic image of a coacervate. Positively and negatively charged polymers spontaneously clump together.[14]

1.4. HYBRID SYSTEM

But maybe we could combine the two and create an interesting hybrid system? After all, cells are not just sacks filled with water, salts, and protein, there are all kinds of sub structures in the cell such as mitochondrion, plasmatic reticulum, and the nucleus among others. We could try to make coacervates inside liposomes, and let them act as a proxy for organelles. They then become a sort of membrane-less, synthetic organelles. We would like to study what kinds of interesting behaviours such a hybrid system might exhibit.

1.5. SPECIFIC AIMS

During this project we used two different coacervation systems. One system was composed of poly-L-lisine (pLL) and adenosine triphosphate (ATP) and the other system was based on poly-uridine (poly-U or RNA) and spermine. We induced coacervation inside liposomes at will by adding one of the coacervation components in the external environment of the liposome and letting it travel through pores in the membrane. The pLL/ATP system was based solely on this passive transport, while the RNA/spermine also contained an enzymatic reaction to trigger coacervation.

Further we observed the dynamics of these systems and obtained the relevant timescales of the coacervation process.

Lastly we proped the possibility to sequester bio-molecules inside the coacervate. We took a look at DNA which is responsible for the storage of genetic information, FtsZ which is an important protein involved in the division process in bacterial cells, small unilameral vesicles (SUVs) which are a potential candidate for liposome growth, and β-galactosidase/fluoroscein which is an enzymatic reaction.

2

Materials and Methods

The general flow of experiments is as follows. First we make liposomes, afterwards we collect them in a chamber on the same chip and then we introduce a feed solution to see the effect of this over time.

2.1. Octanol-assisted Liposome Assembly

To make liposomes we used a technique called Octanol-assisted Liposome Assembly (OLA).[15] OLA uses a microfluidic device to create liposomes that are unilamelar, mono-disperse and have high encapsulating efficiency. These microfluidic devices are made by pouring polydimethylsiloxane (PDMS) on a silicon wafer which has the device design etched into it, bonding it to a PDMS-covered glass slide, and PVA-treating it to make the channel hydrophyllic. A protocol on the specifics of device making can be found in [15]. A schematic overview of the device can be found in figure 2.1.

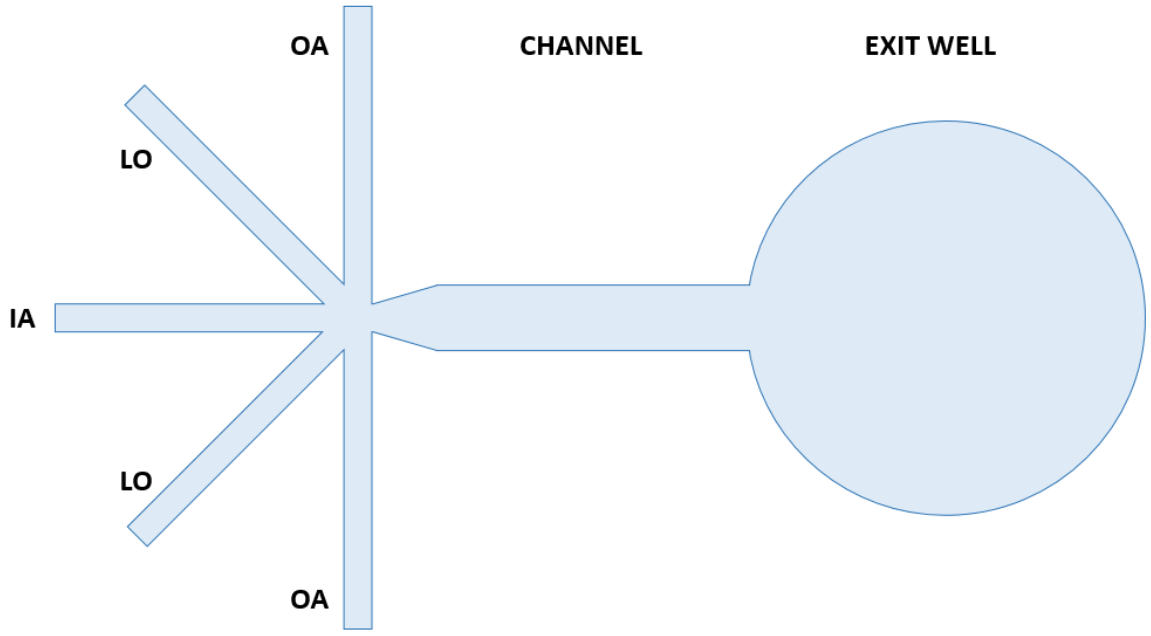

Figure 2.1: Schematic image of the microfluidic device. It consists of transport channels for the outer aqueous phase (OA), the inner aqueous phase (IA), and the Lipid-carrying organic phase (LO). It further contains a channel and an exit hole.

For OLA, three different solutions are pumped into the device using a pressure pump: Inner Aqueous phase (IA), Outer Aqueous phase (OA), and Lipid-carrying Organic phase (LO). The inner aqueous phase contains what will become the inner contents of the liposome. The lipid phase will self-assemble to form a lipid bilayer. The outer aqueous will form the external environment of the liposomes in the channel. Most

significantly, the inner aqueous phase contains something that can form a coacervate (eg. poly-L-lysine), α-hemolysin to form pores, and dextran to make it heavier then it's surroundings. The outer aqueous contains a surfactant (P188) to help form double emulsions. Other chemicals such as buffers and salts can also be present. For the liposome to be stable it is important that there is no osmotic difference between inside and outside. Glucose was used to balance the osmolarity of the inner aqueous phase with the outer aqueous phase and the exit solution. A comprehensive overview of all solutions used during each experiment can be found in the Appendix.

These three solutions flow through the input channels and meet at the junction where at first double-emulsion droplets are formed. These droplets travel through the channel for a few minutes until the pockets separate, and matured liposomes are created. This process is graphically shown in figure 2.2. After the 1-octanol pockets are separated the liposomes leave the channel and enter the the collection site. There are multiple approaches to purifying 1-octanol pockets from liposomes but the approach taken in this project was creating a large well at the end of the channel. In this well, octanol pockets will flow to the surface due to them being lighter than the exit solution, while the liposomes will sink due to them being heavier. This is shown in figure 2.3.

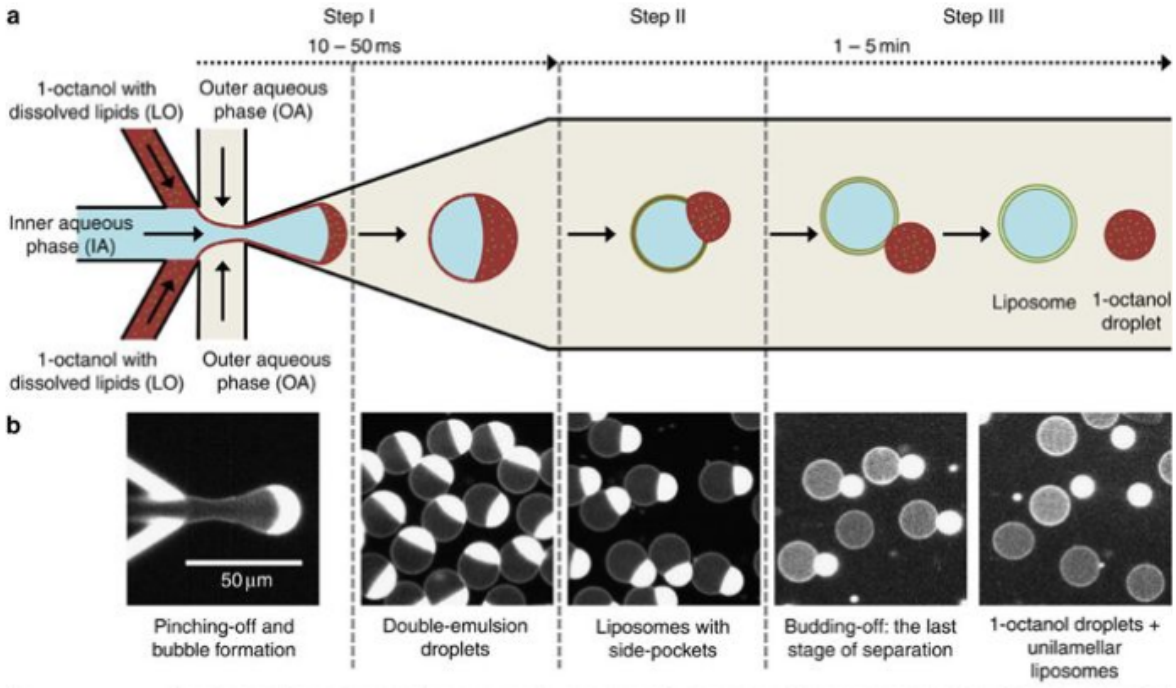

Figure 2.2: a.) The OLA process consists of 3 steps. First double-emulsion droplets are made. Secondly the octanol forms into a pocket. Lastly this pocket releases from the liposome b.) Corresponding fluorescence images to these stages [15].

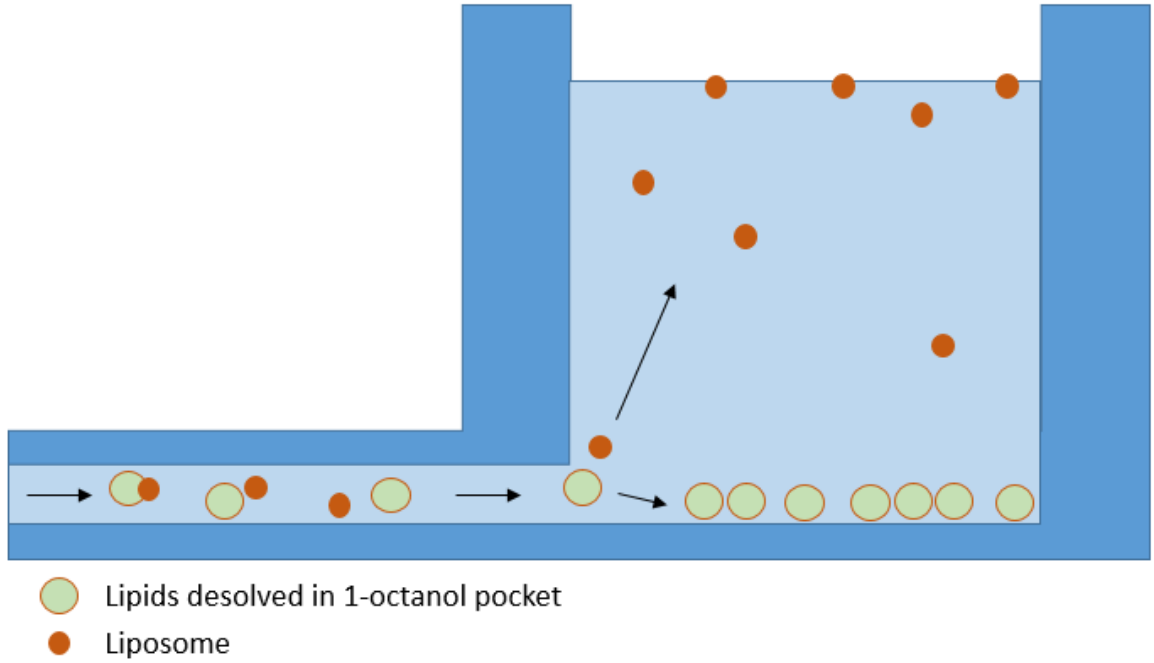

Figure 2.3: Schematic of liposomes settling in the well. Octanol pockets will separate under influence of the flow in the channel. In the exit well octanol pockets will float to the top of the well while liposomes will settle at the bottom.

2.2. INTRODUCING FEED SOLUTION

After the liposomes have settled in the collection well feed solution was pipetted to the well. While doing this, one should be careful not to introduce a significant flow. Minimising flow is of utmost importance to be able to follow the same liposome over any significant period since it is not possible to track liposomes with the current set up. They may therefore flow out of the field of view. The way we found to introduce the least amount of disturbance was to hold the pipette above the exit well and slowly form a droplet of feed solution at the tip of the pipette, then carefully moving the pipette to touch the surface of the exit solution to let it combine. The feed was added after sufficient liposomes where created so we could study the coacervation process real time from the start, for tens of liposomes. If the time zero of the experiment was not required the feed was already included in the exit solution and therefore no flow was introduced..

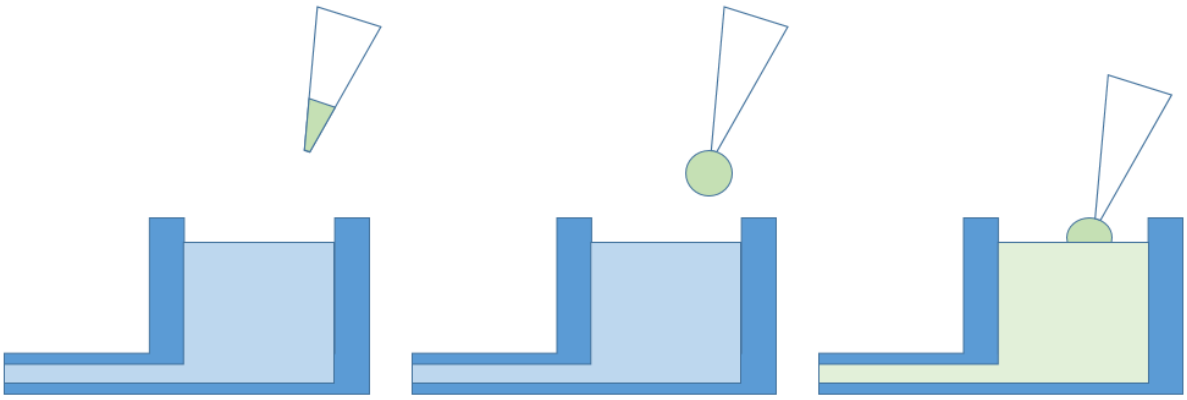

Figure 2.4: Schematic of pipetting method. First the feed is collected at the tip of the pipette. Then this droplet is gently pushed against the surface of the exit solution.

2.3. MICROSCOPY SETUP

During the setup phase of the experiment and the establishment of the production, a 10x or 20x air objective was used due to its larger field of view. During the actual imaging a 60x oil objective was used because of its higher image quality and smaller depth of field, meaning its possible to see a thinner slice of the liposome. We always focused on the equator of the liposome. The microscope that was used is the Olympus IX81 inverted microscope equipped with epifluorescence illumination. MicroManager 1.4.14 was used to control the microscope and acquire images.

2.4. ANALYSIS

FIJI (extension of ImageJ) was used to load the .tif files that were produced by the microscopy setup and to preform principal image manipulation such as creating false color images. For the rest of the analysis MATLAB 2017B was used.

3

Results and Discussion

In studying the coacervate-in-liposome hybrid containers, we assessed two different systems. In the first system coacervation was induced by passive transport of small components through the α-hemolysin pores embedded in the lipid membrane. In the second system, coacervation was achieved through passive transport through the membrane pores as well as an active polymerisation of the ingoing components by a encapsulated enzyme.

3.1. Formation of poly-L-lysine/ATP coacervates inside liposomes

In the passive transport system coacervates were composed out of poly-L-lysine (pLL) and adenosine triphosphate (ATP). The pLL remained confined inside the liposome since it was too large to move through the pores. ATP was added to the collection well after which it quickly diffused throughout the well and entered through the pores. After the ATP had entered the liposome in sufficient quantities coacervation took place. A fraction of the pLL molecules were fluorescently labelled to track the process. A schematic of the coacervation process is given in figure 3.1.

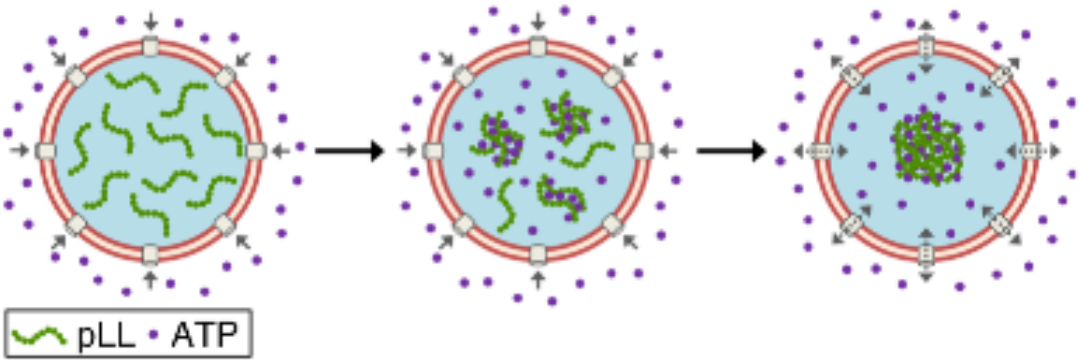

Figure 3.1: pLL/ATP coacervation process. ATP moves through pores and enters the liposome. Here it will start the coacervation process. Over time coacervates coalesce into one big coacervate [16].

Firstly we wanted to show that ATP can indeed travel through the membrane and form coacervates inside the liposome with pLL. We also wanted to see if we could capture the coacervation process from start to finish. We did this by introducing ATP in feed solution. In the experiment we used cy5-pLL to make the coacervation process visible. In figure 3.2 a time-lapse for the pLL/ATP system is shown starting immediately after the introduction of ATP into the collection well.

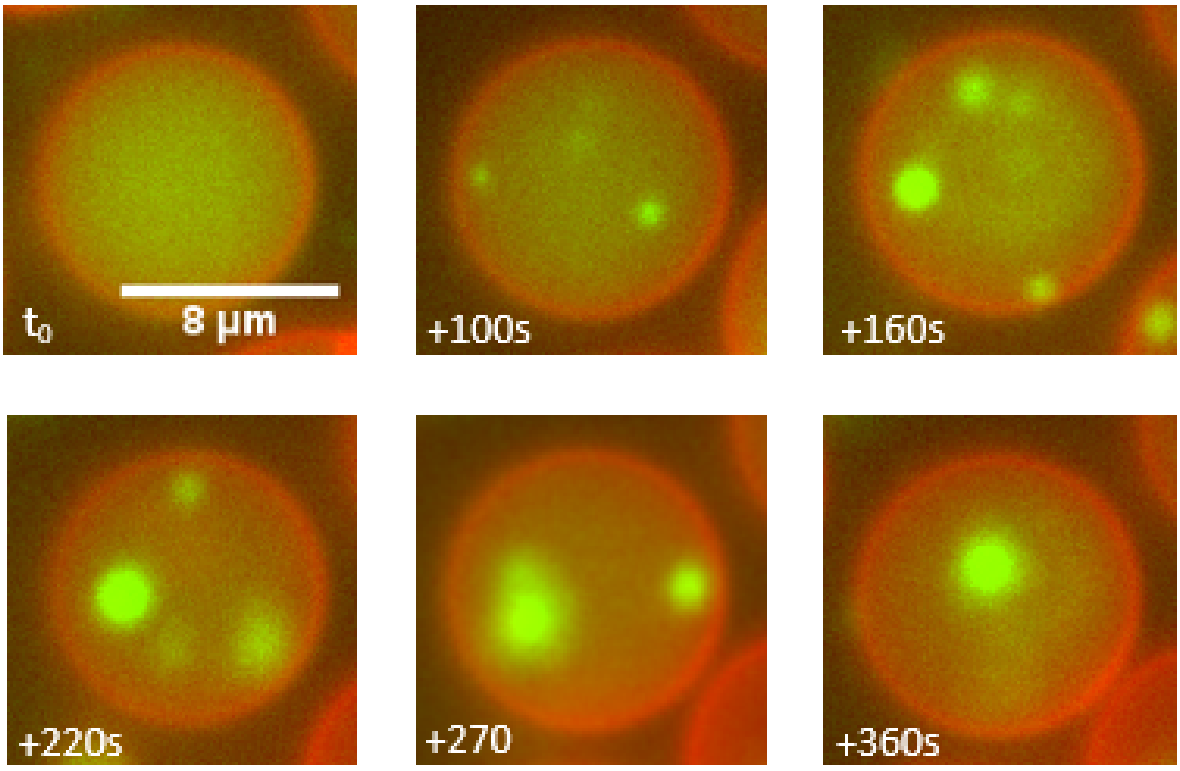

Figure 3.2: Time-lapse of the coacervation of pLL and ATP after addition of ATP to the well (t_0). In this image red signifies rhodanine-lipids and green signifies cy5-pLL.

These images lead us to conclude that ATP indeed induces coacervation inside the liposome. At t_0 the pLL is homogeneously distributed across the liposome. At +100s the first signs of coacervation occur. At +160s most of the pLL is already inside the coacervate phase. The rest of the images mainly shows coacervates coalescing until they all fuse into one coacervate at +360s. To give further evidence that ATP truly moves through the pores and gets inside the coacervate phase an experiment was preformed in which ATP also was fluorescently labelled with cy5 dye. Coacervation was first started with non-labelled pLL. Fluorescently labelled ATP was added to the well. Results are given in figure 3.3

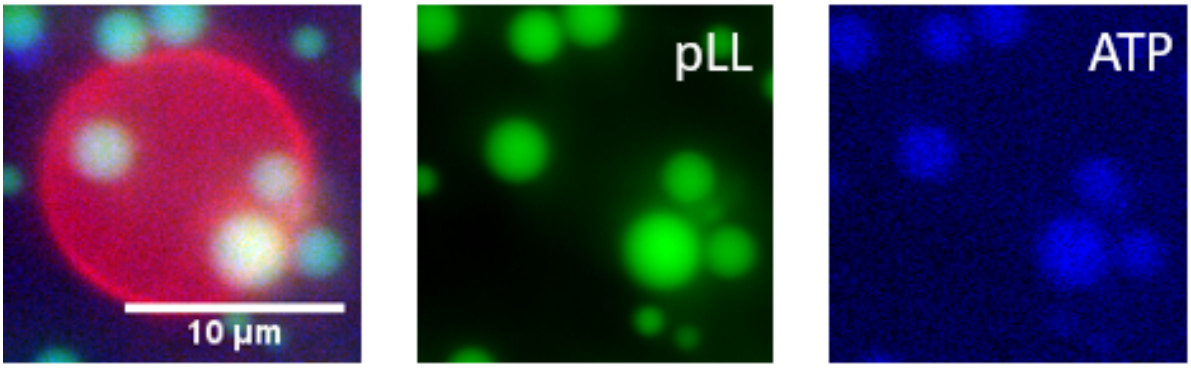

Figure 3.3: Image after coacervation has occurred after adding cy5-ATP to the well. The separate channels for FITC-pLL (green) and cy5-ATP (blue) are also given. It can clearly be seen that FITC-pLL and cy5-ATP are co-localised.

Image quality is not ideal since there are a lot coacervates outside crowding the view. This can happen if there has been a lot issues in the beginning of the OLA process causing a lot of inner aqueous to leak into the exit hole. However it still can be seen from this image that pLL and ATP are indeed co-localised. This further

proofs that ATP can travel through the α-hemolysin pores and that the coacervation indeed occurs between pLL and ATP.

We also want to check that the dextran we are using to weigh down our liposomes doesn't interfere with the coacervates. To check this we added fluorescently labelled dextran to our liposomes and looked at distribution across the liposome. This can be seen in figure 3.4

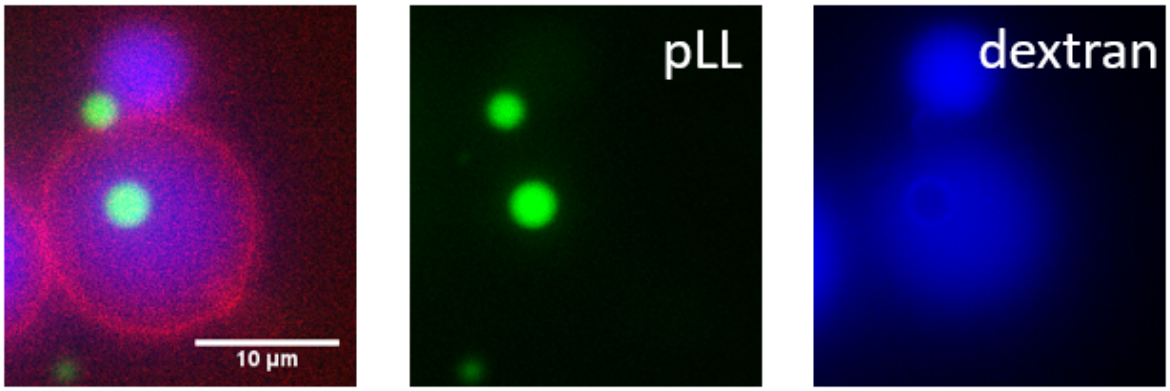

Figure 3.4: Composite fluorescent image of pLL-ATP coacervation with fluorescent dextran. Red is rhodanine-lipids, green is FITC-pLL and blue is cy5-dextran. Separate channels of FITC-pLL and cy5-dextran are also given. A build up of dextran can be observed around the interface of the coacervate.

The top coacervate in figure 3.3 is outside the liposome and is therefore a result of non-ideal liposome production. We can see that dextran is relatively uniformly distributed across the liposome. However there is also a build up visible on the interface of the coacervate. Since coacervates still are able to fuse without any problems, we can conclude that this surface build up of dextran has no effects on the coacervation process.

3.2. EFFICIENCY

We define the efficiency to be the total amount of liposomes with coacervates inside divided by the total amount of liposomes produced. We found it to be 72%±18% by counting 1948 liposomes. Liposomes that don't show coacervation could occur because of bursting and resealing events in which the liposome loses a part of it's inner contents. Improper assembly of α-hemolysin in the membrane could also cause coacervation not to happen.

3.3. MONODISPERSITY

Lastly we want to look at the monodispersity of our liposomes and coacervates. For we manually measured the area of 213 liposomes and coacervates. We found a mean diameter for liposomes of $D_{liposomes} = 14.2 \pm 1.0\mu m$ and a diameter for coacervates of $D_{coacervates} = 2.8 \pm 0.3\mu m$. This gives us a coefficient of variation of $c_{liposomes} = 7.0\%$ and $c_{coacervates} = 10.7\%$. For the intends of this thesis this is monodisperse enough.

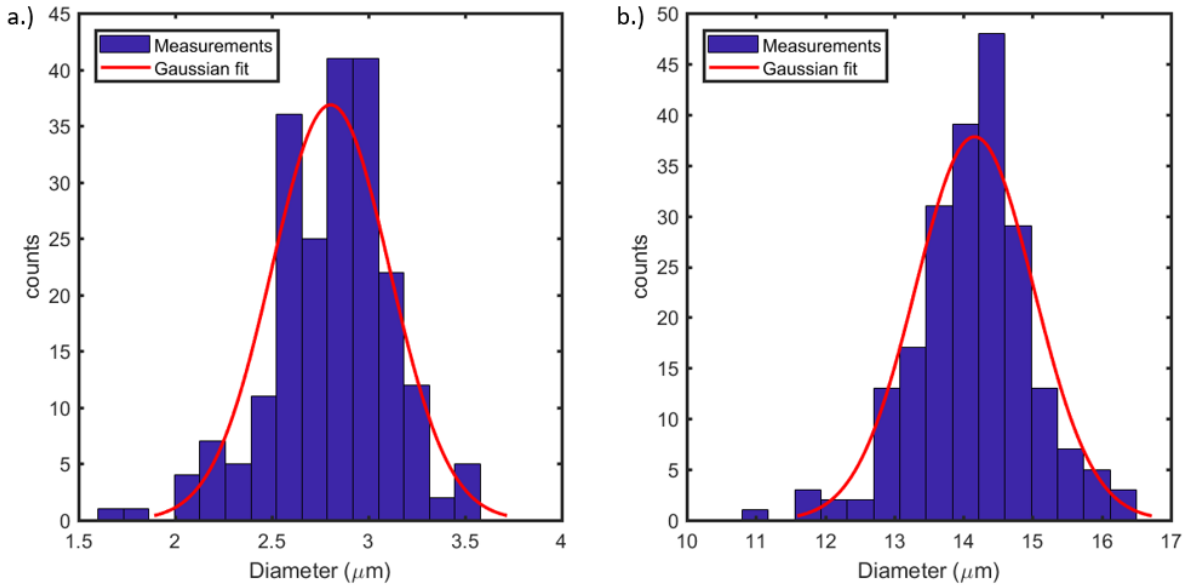

Figure 3.5: Distribution of diameter with a Gaussian fit for a.) coacervates and b.) liposomes

3.4. FORMATION OF RNA/SPERMINE COACERVATES INSIDE LIPOSOMES

Now we will take a look at our second coacervation system. The enzymatically induced coacervation scheme is relatively more complicated. In this system uridine diphosphate (UDP) passes through pores in the membrane to enter the liposome. Here UDP is reduced to uridine monophosphate (UMP) by the enzyme PNPase. As UMP is produced it polymerises with uridine-20 (U-20) seeds to form poly-uridine (poly-U). Lastly, Poly-U forms a coacervate with the spermine already present in the liposome. The U-20 seeds were fluorescently labelled to keep track of the coacervation. An overview of the process is given in figure 3.6.

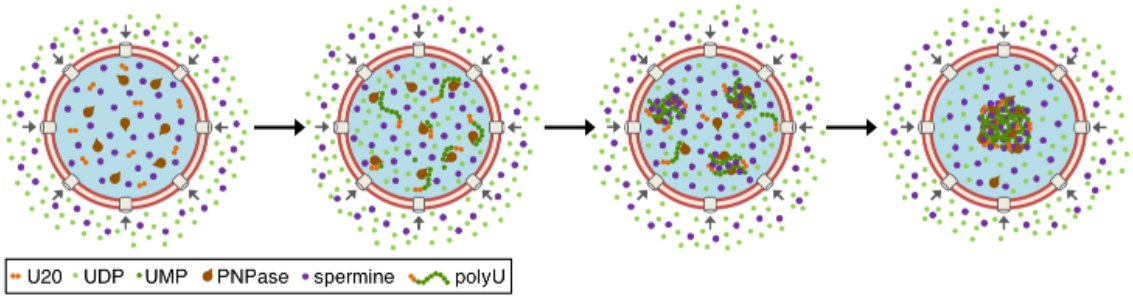

Figure 3.6: RNA/spermine coacervation process. First UDP enters the liposome through the pores. Then PNPase converts UDP to UMP. UMP will polymerise with U-20 seeds to forum poly-U. This happens contentiously as long as UMP is produced and U-20 seeds are available. Poly-U forms coacervates with spermine and over time these will coalesce to form one coacervate.[16]

We then did experiments to find out if this system indeed works. We added a feed solution with ADP to start the coacervation process. The experiments have been done by Kasper Spoelstra and Siddarth Deshpande. Results of the experiment are shown in figure 3.7.

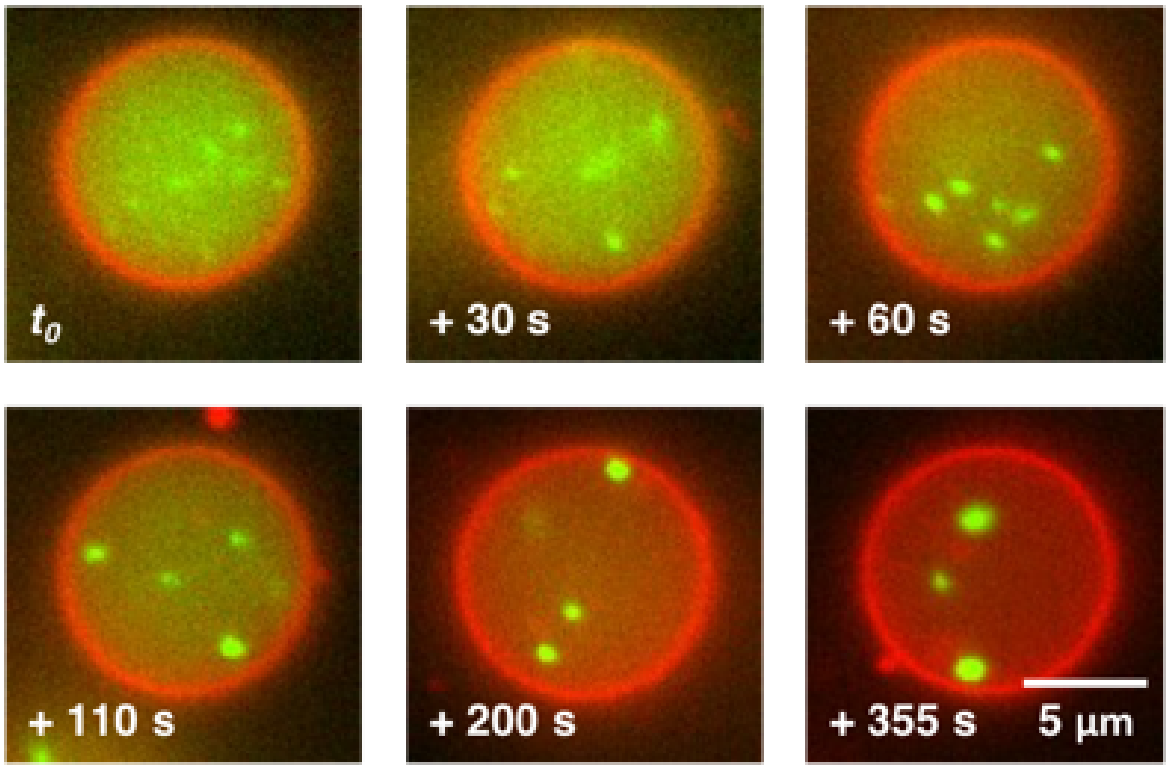

Figure 3.7: Time-lapse of the coacervation of RNA and spermine after addition of ADP to the well (t_0). In this image lipids are shown as red and U-20 seeds are shown as green.[16]

3.5. DYNAMICS OF COACERVATES IN LIPOSOMES

3.5.1. PLL/ATP

Next we wanted to characterise the coacervation dynamics and find the relevant timescales. We did this by looking at two different measures. First we took a threshold of a certain pixel value for which everything above we deem to be inside a coacervate. We then collect the total amount of fluorescence counts inside the coacervate phase. To represent the background fluorescence we took the total fluorescence counts of all pixels below this threshold. We would expect the fluorescence of the coacervates to go up and consequently the fluorescence of the background to go down.

When studying this for the pLL/ATP system data was used provided by Anson Lau. In this data set the liposomes where almost completely stationary which eased the process of analysis. The liposome boundary was taken as a mask to remove everything outside using FIJI (and extension of ImageJ). The pLL channel was then taken and exported to MATLAB plot the desired measures. These are shown in figure 3.8.

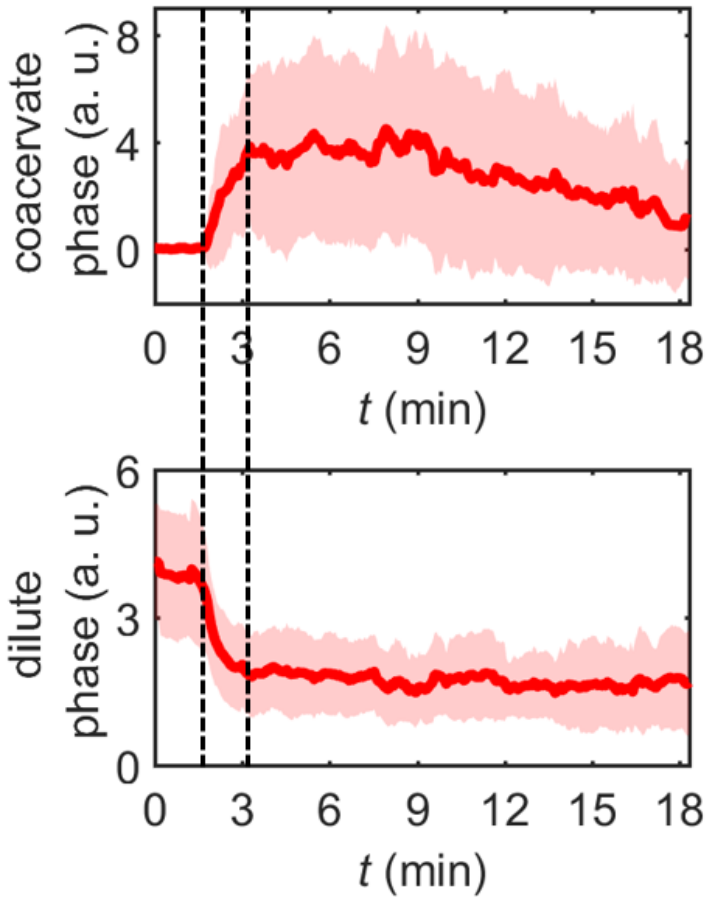

Figure 3.8: Graph of the coacervate phase and dilute phase for ATP/pLL system. At the first dashed line the coacervation start. At the second dashed line it is done.

We can see at dashed vertical line in figure 3.8 that the coacervate phase appears quite sudden. This is in accordance with what we see in the time-lapse (see figure 3.2). We can see that after approximately 1.5 minutes the fluorescence in the coacervate phase plateaus again. The large increase in the error after coacervation is due to the coacervates moving into and out of focus, which can be seen as the large shaded area in figure 3.8. As expected, we can also see a corresponding drop in the background phase at roughly same time as the coacervate phase increases. After approximately 9 minutes, we can see figure 3.8 that the coacervate phase fluorescence starts dropping again. This is likely caused by coacervates settling over time a the bottom of the liposome due to being relatively heavy. This causes them to be out of focus and therefore we see a drop in fluorescence. We do not see any drop in the dilute phase which suggest that there was no significant bleaching during the experiment.

The experiments for which the figure 3.8 is made also contained apyrase inside the liposome. Apyrase converts ATP to AMP a should be able to dissolve the coacervate. However this was not observed during the experiment, possibly because ATP from the collection well could keep flowing inside the liposome through the α-hemolysin pores faster then apyrase could convert them to AMP. Because of the good image quality and amount of liposomes in the field of view this experiment still has been used to produce the coacervation dynamics. A experiment of lower quality but without apyrase is shown in figure **??** to proof the dynamics are similar.

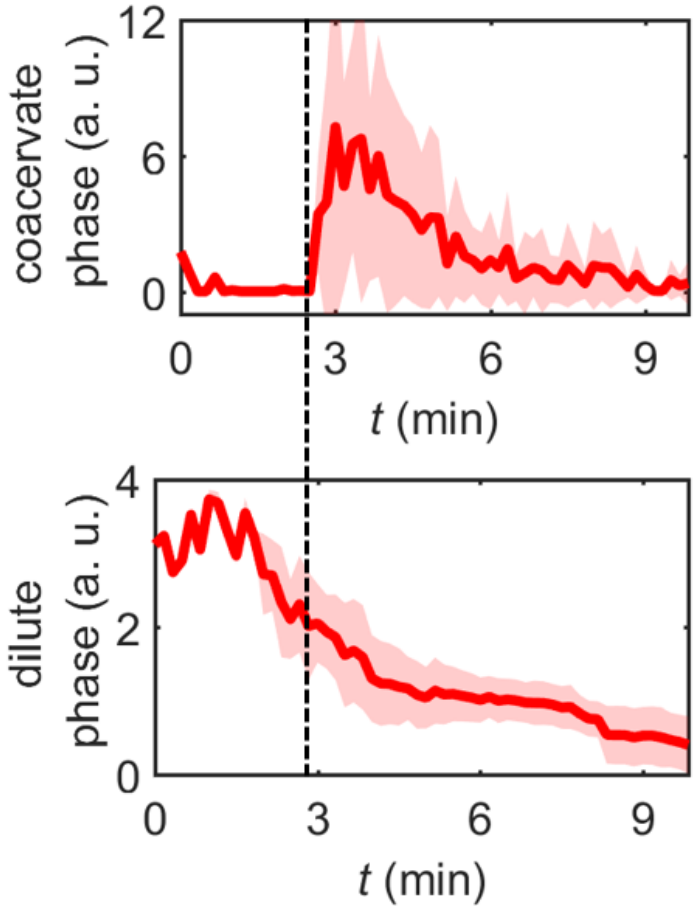

Figure 3.9: Graph of the coacervate phase and dilute phase for ATP/pLL system without apyrase.

3.5.2. RNA/SPERMINE

The same analysis was done on the RNA/spermine system. The analysis of RNA/spermine was much more challenging due to relatively high flow induced by the adding of the feed. This gave rise to the need for tracking liposomes. This was first attempted by using a plug-in for FIJI called TrackMate. However this did not gave the tools needed for our analysis. With TrackMate is was possible to draw the paths of liposomes on the image; however, there was no apparent way to export these xy-positions and use them to crop the image to include only one liposome per image. It was then decided to manually crop the images. However in these image the liposomes were still moving which made it difficult to remove the background. It was then attempted to stabilise the image using another FIJI plug-in called HyperStackReg. This did stabilise the image but not to the degree necessary for our analysis. In the end it was decided to remove the outside of the liposome manually slice by slice, which took a significant amount of time. The result of the analysis can be found in figure 3.10

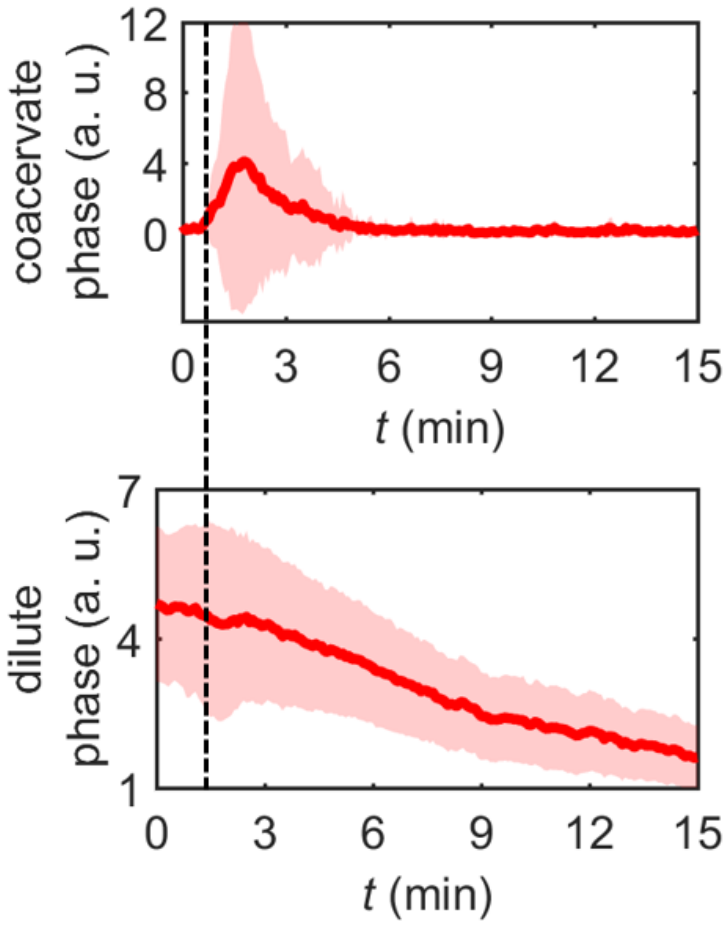

Figure 3.10: Graph of fluorescence coacervate phase and dilute phase for RNA/spermine

If we look at the fluorescence counts of the coacervate phase we now something strange. At first we see a rising line as expected but after around 2 minutes we see the signal going down again until it again goes back to a value close to zero. This could be explained by the fact that over time coacervates tend to sink which means they get out of focus. However towards the end the coacervates are still in focus some of the time (as can be seen in figure 3.7, which is not really seen in the graph. Bleaching could be another explanation, but seems unlikely since in other experiments bleaching is not observed while using similar fluorophores and exposures. Another explanation could be quenching. Over time the coacervate could become more dense, leading them to have higher quenching and therefor lower fluorescence counts. If we look at the dilute phase we see the effect we would expect. PNPase steadily converts UDP in UMP which means that U-20 seeds will slowly enter the coacervate over a longer period of time instead of very sudden as was case with pLL/ATP. We also see that dilute phase doesn't completely plateau, meaning the process is not yet completed. We can therefore say that coacervation takes at least 15 minutes, but could go on for longer. Also if we look at the amount of counts lost in the dilute phase compared to the ones gained in the coacervate phase we see at least a mismatch of one order of magnitude. This could be explained by the aforementioned quenching. Another explanation could be U-20 seeds leaving the liposome via the α-hemolysin pores.

3.6. SEQUESTRATION IN COACERVATES

Lastly we wanted to show that we can sequester different biomolecules inside coacervates. Firstly we wanted to look if we can sequester FtsZ. FtsZ is plays an important role in cell division of bacterial cells. Next we looked if small unilamaler vesicles can be sequestered by coacervates. SUVs could potentially let a liposome grow by fusing to membrane. Thirdly we looked at β-gelactosidase. β-gelactosidase is an enzyme that converts β-gelactosides into monosacharides. We use fluoroscein di-β-D-galactopyranoside (FDG), which fluoresces when cleaved by β-gelactosidase to show the progression of this reaction. Lastly we took a look at DNA, the carrier of genetic information.

3.6.1. FTSZ

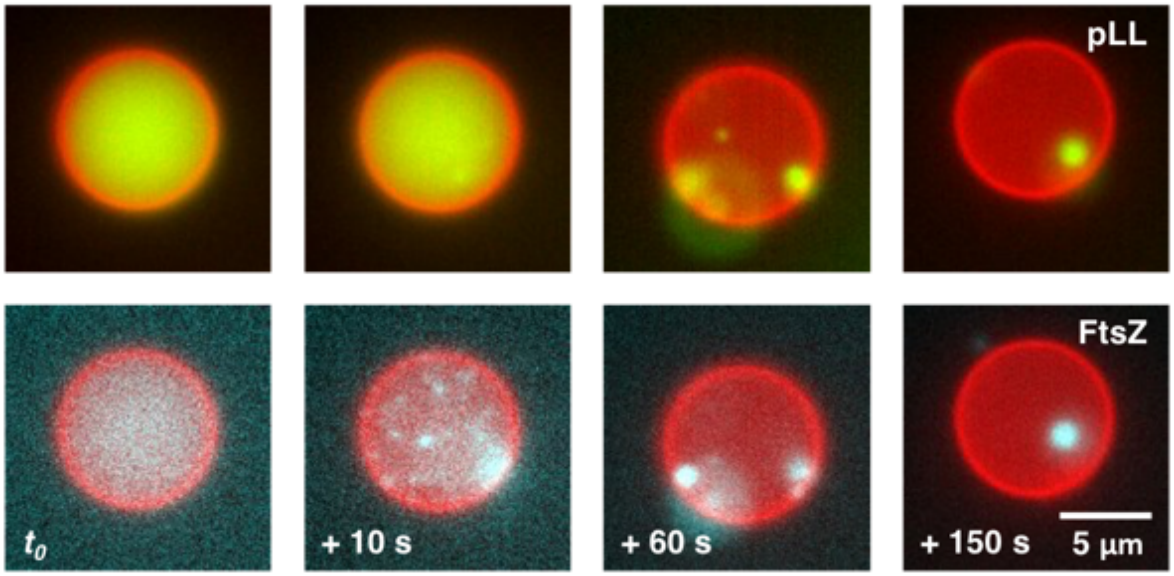

Figure 3.11: Time-lapse of coacervation of pLL (green) and FtsZ (blue). pLL and FtsZ are co-localised.[16]

During this time-lapse it can be nicely seen that pLL and FtsZ are co-localised. As soon as pLL starts coacervation FtsZ gets sequestered inside. At +150s FtsZ is sequestered into one coacervate. There is still a low concentration outside of the coacervate.

3.6.2. SUVS

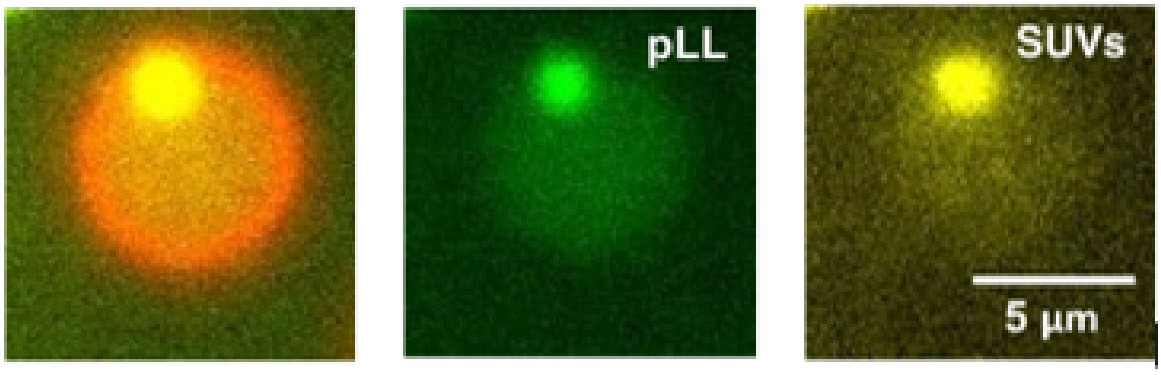

Figure 3.12: Time-lapse showing sequestration of SUVs. Separate channel for pLL (green) and SUVs (yellow) are also given.[16]

SUVs also get sequestered inside the coacervate.

3.6.3. β-GALACTOSIDASE/FLUOROSCEIN

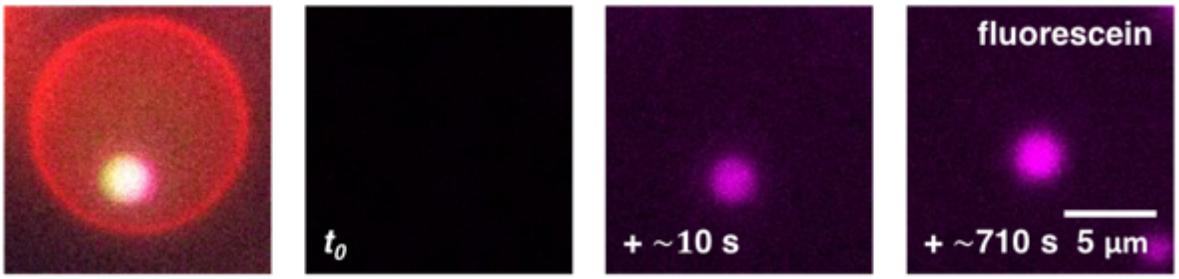

Figure 3.13: Image showing sequestration of fluorescein. At t_0 no fluorescence is observed. After 10s fluorescein fluorescence doensn't increase significantly in intensity.[16]

In the β-galactosidase experiment an attempt was made to show the reaction speed inside versus outside the coacervate, however the reaction was over so fast (after 10 seconds or 1 frame) that no conclusive data on this could be given.

3.6.4. DNA

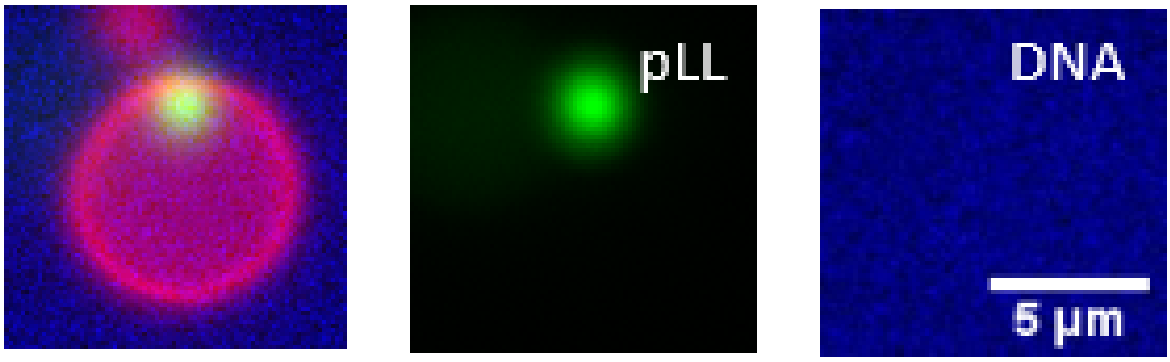

Figure 3.14: Image of liposomes containing pLL/ATP coacervates and DNA. pLL (green) and DNA (blue) channels are given separately. DNA channel seems homogeneous but also very low intensity.

The DNA channel in this experiment seems homogeneous. However the intensity was also very weak (around the same order as the background noise). To get conclusive data about whether or not DNA is sequestered inside coacervates the experiment should be repeated with a higher concentration of fluorescent DNA.

For all experiment the partition coefficient was calculated. This was done by dividing the mean intensity inside the coacervate by the mean intensity of the liposome (but excluding the coacervate) after subtracting the background from both sides.

$$C_{partition} = \frac{I_{coacervate} - I_{background}}{I_{liposome} - I_{background}} \tag{3.1}$$

The results are given in table 3.1.

	Partition Coefficient	Standard Deviation	N
FtsZ	14.2	3.8	25
SUVs	2.9	0.6	35
β-Galactosidase	2.4	0.4	31

Table 3.1: Overview of different partition coefficient for FtsZ, SUVs and β-galactosidase.

We can see that FtsZ has a significantly higher partition coefficient compared to SUVs and β-galactosidase. This signifies that it is easier for FtsZ to enter the coacervate compared to SUVs and β-galactosidase. For SUVs this is possibly due to the large size (30 nm) making it less energetically favourable to be inside the coacervate. Fluorescein is much shorter then FtsZ and might therefore also be less attracted to get in the coacervate.

4

CONCLUSION

We successfully accomplished our aim to build hybrid coacervate-in-liposome systems. We have shown that we can induce this coacervation by adding an external component to the environment of the liposome which then travels through α-hemolysin pore embedded in the membrane. We have done this for both the pLL/ATP and RNA/spermine system. We were able to produce these hybrid systems with a efficiency of 72%±18% (N=1948). The liposomes we create are monodisperse. They have an average diameter $D_{liposomes} = 14.2 \pm 1.0\mu m$ and a diameter for coacervates of $D_{coacervates} = 2.8 \pm 0.3\mu m$ (N=213).

After this we looked at the dynamics of the two systems. We found that pLL/ATP coacervation has a typical coacervation time of 1.5 minutes. We saw that after 9 minutes coacervates began settling at the bottom and became out of focus.

In the RNA/spermine system coacervation took at least 15 minutes. Experiments with a longer time span might have to be done to better understand the dynamics of this system. We saw that the fluorescence of the coacervate phase began dropping after 2 minutes. This could be due to bleaching, however this seems unlikely given that we saw no evidence of bleaching in the pLL/ATP experiment. Quenching due to increased density of the coacervates over time might be a more feasible explanation. It may be important to do an experiment to validate whether or not U-20 seeds can move through the α-hemolysin pores, since it is critical for the experiment that this does not happen.

We conclude that hybrid coacervation-in-liposome systems can sequester FtsZ (important in bacterial cell division) with partition coefficient 14.2 ± 3.8, SUVs (potential candidate for cell growth) with partition coefficient 2.9 ± 0.6, and β-galactosidase/fluoroscein (enzymatic reaction) with partition coefficient 2.4 ± 0.4. We would have liked to study the difference in reaction rate of β-galactosidase inside the coacervate compared to outside but the reaction was completed too fast (10s) for our set-up to measure it.

5

RECOMMENDATIONS

It would be nice if we could better follow liposomes during the coacervation process. One of the most important issues to combat is the introduction of flow by pipetting during the experiment. The total amount feed solution to be added was already lowered from being equal to the exit hole solution to being one tenth of the exit hole solution. A pipetting scheme for introducing as little flow as possible has been mentioned in Materials and Methods. However flow still cannot be completely eliminated. One solution is to further lower the amount feed added by using higher stock solutions. However there is a limit to how small an amount still can be pipetted accurately.

An alternative solution might be using support grids used in transmission electron microscope (TEM). These are copper grids that are roughly the size of our exit whole and roughly the height and size of our liposomes.

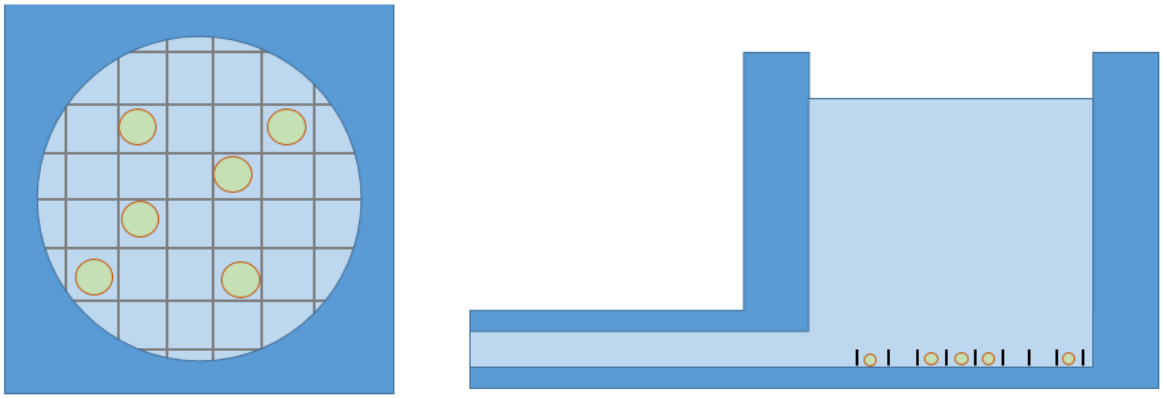

Figure 5.1: Schematic of a copper TEM-grid inside the exit hole. The grid will sit on the bottom and liposomes will settle inside, stopping them from moving across the surface.

These grids could hamper flow in the bottom regions of the exit well or at least confining the liposomes to one field of view. How these grids should be implemented in the current device is could be subject of further research since they are very fragile.

Another solutions could be making the exit hole much smaller. Currently large parts of the exit hole are empty under normal production. This means that the liposomes are totally free to move. Adding feed to the collection hole doesn't seem to introduce any flow in the z-direction, or it is so weak that its not able to lift the liposomes. The flow we observe is almost always in the xy-plane. If the liposomes would therefore be tightly packet, they would be able to move laterally anymore. We could achieve this by decreasing the area of the collection well until it can easily be filled with liposomes. Multiple layers of liposomes could even increase the stability. Currently the well is 4 mm in diameter. Ideally this would be reduce as much as possible while still being able to pipette in a feed solution.

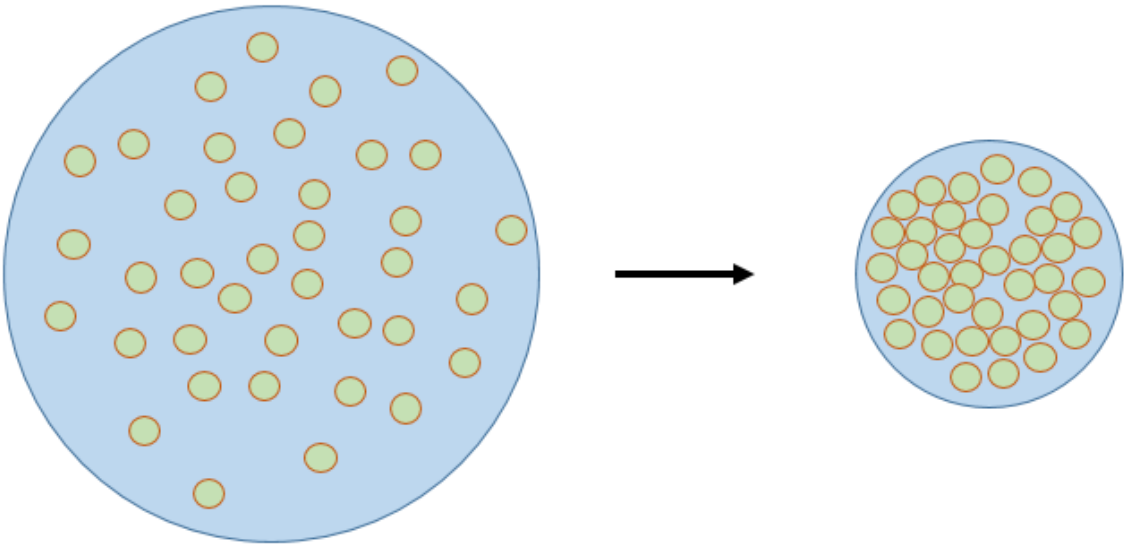

Figure 5.2: Moving for large to small well.

Also it might be advisable to more stringently look for software that can successfully track liposomes. If no software can be found its also possible to develop custom software/edit existing software to track liposomes. A significant part of the analysis for this report was spent on manually tracking liposomes. If this could be automatised, more time could be spent on more productive tasks.

We have shown that coacervates can sequester different kinds of molecules. However it would also be nice to be able to dissolve the coacervate again and make the sequestered chemicals available in the liposome. This could be done using apyrase which converts ATP, which forms coacervates, to AMP which doesn't form coacervates. This has been shown to work in bulk. However when we put apyrase inside a liposome coacervates do not get disolved. This is hypothesised to be due the abundance of ATP available in the exit well which acts like a infinite reservoir (>10^3 times larger then volume of all liposomes). Apyrase does convert ATP to AMP but ATP keeps flushing in from the outside environment. To get rid of this ATP we could also pipet a small amount of apyrase to the environment. After this the coacervate will dissolve and it's contents become freely available. If ATP is added again the coacervation process start over again until apyrase has converted enough ATP again for the coacervate to dissolve. This gives us control over the release and sequestration of certain chemicals inside the liposome.

The next step would be to be able to make two separate coacervates inside a liposome that can both be dissolved at will. If such a system is achieved we could for instance first release SUVs to let the liposome grow. When the liposome has grown enough we can sequester the SUVs again. Then we can release chemicals to divide the liposome, for instance FtsZ. This would liposomes that could grow and reproduce, albeit not autonomously. This would be a very exciting system!

A

EXPERIMENTS

EX1 30/04/2018 pLL no ATP

Inner aqueous	Stock Concentration (mM)	Final concentration (mM)	Dissociation Factor	Osmolarity (mOsm)	Volume to add (uL)
Sucrose	1000	100.00	1	100.00	10.0
Glycerol	100%	0.15	0	0.00	15.0
KCl	1000	150.00	2	300.00	15.0
MgCl2	1000	5.00	3	15.00	0.5
pLL	2.22	0.21	155	32.72	9.5
cy5pLL	0.16	0.01	1	0.01	6.3
TrisHCl	1000	25.00	1	25.00	2.5
H2O					41.2
Total				472.73	100.0

Outer aqueous	Stock Concentration (mM)	Final concentration (mM)	Dissociation Factor	Osmolarity (mOsm)	Volume to add (uL)
Glucose	1000	132.73	1	132.73	13.3
Glycerol	100%	0.15	0	0.00	15.0
KCl	1000	150.00	2	300.00	15.0
MgCl2	1000	5.00	3	15.00	0.5
TrisHCl	1000	25.00	1	25.00	2.5
P188	10000	5000.00	0	0.00	50.0
H2O					3.7
Total				472.73	100.0

Exit hole solution	Stock Concentration (mM)	Final concentration (mM)	Dissocation Factor	Osmolarity (mM)	Volume to add (uL)
Glucose	1000	132.73	1	132.73	13.3
Glycerol	100%	0.15	0	0.00	15.0
KCl	1000	150.00	2	300.00	15.0
MgCl2	1000	5.00	3	15.00	0.5
TrisHCl	1000	25.00	1	25.00	2.5
H2O					53.7
Total				472.73	100.0

Glucose = osmotic compensator

EX2 18/05/2018 pLL ATP

Inner aqueous	Stock Concentration (mM)	Final concentration (mM)	Dissociation Factor	Osmolarity (mOsm)	Volume to add (uL)
dextran 6000	20	5	1	5	12.50
Glycerol	100%	15%	0	0	7.50
KCl	1000	135	2	270	6.75
MgCl2	1000	5	3	15	0.25
pLL	2.22	0.22	155	34.1	4.95
FITCpLL	0.44	0.02	1	0.02	2.27
TrisHCl	1000	22.5	1.84	41.4	1.13
alpha-hemolysin	0.015	0.0015		34.6	5.00
H2O					9.65
Total				400.12	50.00

Outer aqueous	Stock Concentration (mM)	Final concentration (mM)	Dissociation Factor	Osmolarity (mOsm)	Volume to add (uL)
Glucose	1000	39.12	1	39.12	3.91
Glycerol	100%	15%	0	0	15.00
KCl	1000	150	2	300	15.00
MgCl2	1000	5	3	15	0.50
TrisHCl	1000	25	1.84	46	2.50
P188	10000	5000	0	0	50.00
H2O					13.09
Total				400.12	100.00

Exit hole solution	Stock Concentration (mM)	Final concentration (mM)	Dissocation Factor	Osmolarity (mM)	Volume to add (uL)
Glucose	1000	9.12	1	9.12	0.91
Glycerol	100%	15%	0	0	15.00
KCl	1000	150	2	300	15.00
MgCl2	1000	5	3	15	0.50
TrisHCl	1000	25	1.84	46	2.50
ATP	100	10	3	30	10.00
H2O					56.09
Total				400.12	100

Glucose = osmotic compensator

EX3 04/06/2018 pyrovite kinase

Inner aqueous	Stock Concentration (mM)	Final concentration (mM)	Dissociation Factor	Osmolarity (mOsm)	Volume to add (uL)
Dextran 6000	20	5.00	1	5.00	12.50
Glycerol	100%	0.15	0	0.00	7.50
KCl	1000	135.00	2	270.00	6.75
MgCl2	1000	5.00	3	15.00	0.25
pLL	2.22	0.21	155	32.72	4.75
cy5pLL	0.16	0.01	1	0.01	3.13
pyrovita kinase	5225	418.00	0	0.00	4.00
alpha hemolysin	0.015	0.0015	23067	34.60	5.00
PEP	100	10	2	20.00	5.00
TrisHCl	1000	22.50	1.84	41.40	1.13
H2O					0.00
Total				418.73	50.00

Outer aqueous	Stock Concentration (mM)	Final concentration (mM)	Dissociation Factor	Osmolarity (mOsm)	Volume to add (uL)
Glucose	1000	57.73	1	57.73	5.77
Glycerol	100%	0.15	0	0.00	15.00
KCl	1000	150.00	2	300.00	15.00
MgCl2	1000	5.00	3	15.00	0.50
TrisHCl	1000	25.00	1.84	46.00	2.50
P188	10000	5000.00	0	0.00	50.00
H2O					11.23
Total				418.73	100.00

Exit hole solution	Stock Concentration (mM)	Final concentration (mM)	Dissocation Factor	Osmolarity (mM)	Volume to add (uL)
Glucose	1000	37.73	1	37.73	3.77
Glycerol	100%	0.15	0	0.00	15.00
KCl	1000	150.00	2	300.00	15.00
MgCl2	1000	5.00	3	15.00	0.50
ADP	100	10.00	2	24.60	10.00
TrisHCl	1000	22.50	1.84	41.40	2.25
H2O					53.48
Total				418.73	100.0

Glucose = osmotic compensator

EX4 07/06/2018 pyrovite kinase

Inner aqueous	Stock Concentration (mM)	Final concentration (mM)	Dissociation Factor	Osmolarity (mOsm)	Volume to add (uL)
Dextran 6000	20	5.00	1	5.00	12.50
Glycerol	100%	0.15	0	0.00	7.50
KCl	1000	135.00	2	270.00	6.75
MgCl2	1000	5.00	3	15.00	0.25
pLL	2.22	0.21	155	32.72	4.75
cy5pLL	0.16	0.01	1	0.01	3.13
pyrovita kinase	5225	522.50	0	0.00	5.00
alpha hemolysin	0.015	0.0015	23067	34.60	5.00
TrisHCl	1000	22.50	1.84	41.40	1.13
H2O					4.00
Total				398.73	50.00

Outer aqueous	Stock Concentration (mM)	Final concentration (mM)	Dissociation Factor	Osmolarity (mOsm)	Volume to add (uL)
Glucose	1000	37.73	1	37.73	3.77
Glycerol	100%	0.15	0	0.00	15.00
KCl	1000	150.00	2	300.00	15.00
MgCl2	1000	5.00	3	15.00	0.50
TrisHCl	1000	25.00	1.84	46.00	2.50
P188	10000	5000.00	0	0.00	50.00
H2O					13.23
Total				398.73	100.00

Exit hole solution	Stock Concentration (mM)	Final concentration (mM)	Dissocation Factor	Osmolarity (mM)	Volume to add (uL)
Glucose	1000	-2.27	1	-2.27	0.00
Glycerol	100%	0.15	0	0.00	15.00
KCl	1000	150.00	2	300.00	15.00
MgCl2	1000	5.00	3	15.00	0.50
PEP	100	10	2	20.00	10.00
ADP	100	10.00	2	24.60	10.00
TrisHCl	1000	22.50	1.84	41.40	2.25
H2O					47.25
Total				398.73	100.0

Glucose = osmotic compensator

EX5 06/13/2018 pLL ATP

Inner aqueous	Stock Concentration (mM)	Final concentration (mM)	Dissociation Factor	Osmolarity (mOsm)	Volume to add (uL)
dextran 6000	20	5	1	5	12.50
Glycerol	100%	15%	0	0	7.50
KCl	1000	135	2	270	6.75
MgCl2	1000	5	3	15	0.25
pLL	2.22	0.22	155	34.1	4.95
FITCpLL	0.44	0.02	1	0.02	2.27
TrisHCl	1000	22.5	1.84	41.4	1.13
alpha-hemolysin	0.015	0.0015		34.6	5.00
H2O					9.65
Total				400.12	50.00

Outer aqueous	Stock Concentration (mM)	Final concentration (mM)	Dissociation Factor	Osmolarity (mOsm)	Volume to add (uL)
Glucose	1000	39.12	1	39.12	3.91
Glycerol	100%	15%	0	0	15.00
KCl	1000	150	2	300	15.00
MgCl2	1000	5	3	15	0.50
TrisHCl	1000	25	1.84	46	2.50
P188	10000	5000	0	0	50.00
H2O					13.09
Total				400.12	100.00

Exit hole solution	Stock Concentration (mM)	Final concentration (mM)	Dissocation Factor	Osmolarity (mM)	Volume to add (uL)
Glucose	1000	9.12	1	9.12	0.91
Glycerol	100%	15%	0	0	15.00
KCl	1000	150	2	300	15.00
MgCl2	1000	5	3	15	0.50
TrisHCl	1000	25	1.84	46	2.50
ATP	100	10	3	30	10.00
H2O					56.09
Total				400.12	100

Glucose = osmotic compensator

EX6 14/06/2018 DNA

Inner aqueous	Stock Concentration (mM)	Final concentration (mM)	Dissociation Factor	Osmolarity (mOsm)	Volume to add (uL)
dextran 6000	20	5	1	5	25.00
Glycerol	100%	15%	0	0	15.00
KCl	1000	135	2	270	13.50
MgCl2	1000	5	3	15	0.50
pLL	2.22	0.22	155	34.1	9.91
FITCpLL	0.44	0.02	1	0.02	4.55
DNA	0.000062	0.0000062	0	0	10.00
TrisHCl	1000	22.5	1.84	41.4	2.25
alpha-hemolysin	0.015	0.0015	23067	34.6	10.00
H2O					9.29
Total				400.12	100.00

Outer aqueous	Stock Concentration (mM)	Final concentration (mM)	Dissociation Factor	Osmolarity (mOsm)	Volume to add (uL)
Glucose	1000	39.12	1	39.12	3.91
Glycerol	100%	15%	0	0	15.00
KCl	1000	150	2	300	15.00
MgCl2	1000	5	3	15	0.50
TrisHCl	1000	25	1.84	46	2.50
P188	10000	5000	0	0	50.00
H2O					13.09
Total				400.12	100.00

Exit hole solution	Stock Concentration (mM)	Final concentration (mM)	Dissocation Factor	Osmolarity (mM)	Volume to add (uL)
Glucose	1000	9.12	1	9.12	0.91
Glycerol	100%	15%	0	0	15.00
KCl	1000	150	2	300	15.00
MgCl2	1000	5	3	15	0.50
TrisHCl	1000	25	1.84	46	2.50
ATP	100	10	3	30	10.00
H2O					56.09
Total				400.12	100

Glucose = osmotic compensator

EX7 20/06/2018 DNA

Inner aqueous	Stock Concentration (mM)	Final concentration (mM)	Dissociation Factor	Osmolarity (mOsm)	Volume to add (uL)
dextran 6000	20	5	1	5	12.50
Glycerol	100%	15%	0	0	7.50
KCl	1000	135	2	270	6.75
MgCl2	1000	5	3	15	0.25
pLL	2.22	0.22	155	34.1	4.95
FITCpLL	0.44	0.02	1	0.02	2.27
TrisHCl	1000	22.5	1.84	41.4	1.13
alpha-hemolysin	0.015	0.0015		34.6	5.00
DNA (1.2 kb)	0.000062	0.000012	1	0	9.68
H2O					-0.03
Total				400.12	50.00

Outer aqueous	Stock Concentration (mM)	Final concentration (mM)	Dissociation Factor	Osmolarity (mOsm)	Volume to add (uL)
Glucose	1000	39.12	1	39.12	3.91
Glycerol	100%	15%	0	0	15.00
KCl	1000	150	2	300	15.00
MgCl2	1000	5	3	15	0.50
TrisHCl	1000	25	1.84	46	2.50
P188	10000	5000	0	0	50.00
H2O					13.09
Total				400.12	100.00

Exit hole solution	Stock Concentration (mM)	Final concentration (mM)	Dissocation Factor	Osmolarity (mOsm)	Volume to add (uL)
Glucose	1000	9.12	1	9.12	0.91
Glycerol	100%	15%	0	0	15.00
KCl	1000	150	2	300	15.00
MgCl2	1000	5	3	15	0.50
TrisHCl	1000	25	1.84	46	2.50
ATP	100	10	3	30	10.00
H2O					56.09
Total				400.12	100

Glucose = osmotic compensator
use low-binding tubing for the IA!

EX8 20/06/2018 RNA

Inner aqueous	Stock Concentration (mM)	Final concentration (mM)	Dissociation Factor	Osmolarity (mOsm)	Volume to add (uL)
dextran 6000	20	5	1	5	12.50
Glycerol	100%	15%	0	0	7.50
KCl	1000	135	2	270	6.75
MgCl2	1000	5	3	15	0.25
pLL	2.22	0.22	155	34.1	4.95
FITCpLL	0.44	0.02	1	0.02	2.27
TrisHCl	1000	22.5	1.84	41.4	1.13
alpha-hemolysin	0.015	0.0015		34.6	5.00
RNA (U20-cy5)	0.1	0.001	1	0	0.50
H2O					9.15
Total				400.12	50.00

Outer aqueous	Stock Concentration (mM)	Final concentration (mM)	Dissociation Factor	Osmolarity (mOsm)	Volume to add (uL)
Glucose	1000	39.12	1	39.12	3.91
Glycerol	100%	15%	0	0	15.00
KCl	1000	150	2	300	15.00
MgCl2	1000	5	3	15	0.50
TrisHCl	1000	25	1.84	46	2.50
P188	10000	5000	0	0	50.00
H2O					13.09
Total				400.12	100.00

Exit hole solution	Stock Concentration (mM)	Final concentration (mM)	Dissocation Factor	Osmolarity (mM)	Volume to add (uL)
Glucose	1000	9.12	1	9.12	0.91
Glycerol	100%	15%	0	0	15.00
KCl	1000	150	2	300	15.00
MgCl2	1000	5	3	15	0.50
TrisHCl	1000	25	1.84	46	2.50
ATP	100	10	3	30	10.00
H2O					56.09
Total				400.12	100

Glucose = osmotic compensator
use low-binding tubing for the IA!

EX9 20/06/2018 dextran

Inner aqueous	Stock Concentration (mM)	Final concentration (mM)	Dissociation Factor	Osmolarity (mOsm)	Volume to add (uL)
dextran 6000	20	5	1	5	12.50
Glycerol	100%	15%	0	0	7.50
KCl	1000	135	2	270	6.75
MgCl2	1000	5	3	15	0.25
pLL	2.22	0.22	155	34.1	4.95
FITCpLL	0.44	0.02	1	0.02	2.27
TrisHCl	1000	22.5	1.84	41.4	1.13
alpha-hemolysin	0.015	0.0015		34.6	5.00
DextranAF647	0.04	0.002	1	0	2.50
H2O					7.15
Total				400.12	50.00

Outer aqueous	Stock Concentration (mM)	Final concentration (mM)	Dissociation Factor	Osmolarity (mOsm)	Volume to add (uL)
Glucose	1000	39.12	1	39.12	3.91
Glycerol	100%	15%	0	0	15.00
KCl	1000	150	2	300	15.00
MgCl2	1000	5	3	15	0.50
TrisHCl	1000	25	1.84	46	2.50
P188	10000	5000	0	0	50.00
H2O					13.09
Total				400.12	100.00

Exit hole solution	Stock Concentration (mM)	Final concentration (mM)	Dissocation Factor	Osmolarity (mM)	Volume to add (uL)
Glucose	1000	9.12	1	9.12	0.91
Glycerol	100%	15%	0	0	15.00
KCl	1000	150	2	300	15.00
MgCl2	1000	5	3	15	0.50
TrisHCl	1000	25	1.84	46	2.50
ATP	100	10	3	30	10.00
H2O					56.09
Total				400.12	100

Glucose = osmotic compensator

EX13 06/07/2018 B-galactosidase pLL ATP

Inner aqueous	Stock Concentration (mM)	Final concentration (mM)	Dissociation Factor	Osmolarity (mOsm)	Volume to add (uL)
dextran 6000	20	5	1	5	12.5
Glycerol	100%	15%	0	0	7.5
KCl	1000	135	2	270	6.8
MgCl2	1000	4.5	3	13.5	0.2
pLL	2.22	0.22	155	34.1	5.0
cy5pLL	0.16	0.01	1	0.01	3.1
TrisHCl	1000	22	1.84	40.48	1.1
alpha-hemolysin	0.015	0.0015		34.6	5
beta-galactosidase	1KU in 50% glycerol, 5 mM Tris Cl, 5 mM MgCl2, 0.5 mM DTT, 0.5 mM mercaptoethanol	10		2.52	5
H2O					3.8
Total				400.21	50

Outer aqueous	Stock Concentration (mM)	Final concentration (mM)	Dissociation Factor	Osmolarity (mOsm)	Volume to add (uL)
Glucose	1000	39.21	1	39.21	3.921
Glycerol	100%	15%	0	0	15
KCl	1000	150	2	300	15
MgCl2	1000	5	3	15	0.5
TrisHCl	1000	25	1.84	46	2.5
P188	10000	5000	0	0	50
H2O					13.079
Total				400.21	100

Exit hole solution	Stock Concentration (mM)	Final concentration (mM)	Dissocation Factor	Osmolarity (mOsm)	Volume to add (uL)
Glucose	1000	9.21	1	9.21	0.921
Glycerol	100%	15%	0	0	15
KCl	1000	150	2	300	15
MgCl2	1000	5	3	15	0.5
TrisHCl	1000	25	1.84	46	2.5
ATP	100	10	3	30	10
Fluorescein di-β-D-galactopyranoside (FDG)	10	0	1	1	0
H2O					56.079
Total				400.21	100

Glucose = osmotic compensator
use the low-binding tubing for the IA

EX11 21/06/2018 FtsZ

Inner aqueous	Stock Concentration (mM)	Final concentration (mM)	Dissociation Factor	Osmolarity (mOsm)	Volume to add (uL)
dextran 6000	20	5	1	5	12.5
Glycerol	100%	15%	0	0	7.50
KCl	1000	85	2	170	4.25
MgCl2	1000	4.5	3	13.5	0.23
pLL	2.22	0.22	155	34.1	4.95
cy5pLL	0.16	0.01	1	0.01	3.13
TrisHCl	1000	17.5	1.84	32.2	0.88
alpha-hemolysin	0.015	0.0015		34.6	5.00
FtsZ	100 µM in 500 mM KCl, 50 mM Tris-Cl, 5 mM MgCl2, 10% glycerol	10		110.7	5.00
H2O					6.57
Total				400.11	50.00

Outer aqueous	Stock Concentration (mM)	Final concentration (mM)	Dissociation Factor	Osmolarity (mOsm)	Volume to add (uL)
Glucose	1000	39.11	1	39.11	3.911
Glycerol	100%	15%	0	0	15
KCl	1000	150	2	300	15
MgCl2	1000	5	3	15	0.5
TrisHCl	1000	25	1.84	46	2.5
P188	10000	5000	0	0	50
H2O					13.089
Total				400.11	100

Exit hole solution	Stock Concentration (mM)	Final concentration (mM)	Dissocation Factor	Osmolarity (mOsm)	Volume to add (uL)
Glucose	1000	9.11	1	9.11	0.911
Glycerol	100%	15%	0	0	15
KCl	1000	150	2	300	15
MgCl2	1000	5	3	15	0.5
TrisHCl	1000	25	1.84	46	2.5
ATP	100	10	3	30	10
H2O					56.089
Total				400.11	100

Glucose = osmotic compensator
use the low-binding tubing for the IA

EX12 21/06/2018 SUVs

Inner aqueous	Stock Concentration (mM)	Final concentration (mM)	Dissociation Factor	Osmolarity (mOsm)	Volume to add (uL)
dextran 6000	20	5	1	5	12.50
Glycerol	100%	15%	0	0	7.50
KCl	1000	135	2	270	6.75
MgCl2	1000	5	3	15	0.25
pLL	2.22	0.22	155	34.1	4.95
cy5pLL	0.16	0.01	1	0.01	3.13
TrisHCl	1000	22.5	1.84	41.4	1.13
alpha-hemolysin	0.015	0.0015		34.6	5.00
SUVs	20 mg/mL			0	8.80
H2O					0.00
Total				400.11	50.00

Outer aqueous	Stock Concentration (mM)	Final concentration (mM)	Dissociation Factor	Osmolarity (mOsm)	Volume to add (uL)
Glucose	1000	39.11	1	39.11	3.91
Glycerol	100%	15%	0	0	15.00
KCl	1000	150	2	300	15.00
MgCl2	1000	5	3	15	0.50
TrisHCl	1000	25	1.84	46	2.50
P188	10000	5000	0	0	50.00
H2O					13.09
Total				400.11	100.00

Exit hole solution	Stock Concentration (mM)	Final concentration (mM)	Dissocation Factor	Osmolarity (mOsm)	Volume to add (uL)
Glucose	1000	9.11	1	9.11	0.91
Glycerol	100%	15%	0	0	15.00
KCl	1000	150	2	300	15.00
MgCl2	1000	5	3	15	0.50
TrisHCl	1000	25	1.84	46	2.50
ATP	100	10	3	30	10.00
H2O					56.09
Total				400.11	100.00

Glucose = Osmotic compensator
use the low-binding tubing for the IA

EX13 21/06/2018 B-galactosidase pLL ATP

Inner aqueous	Stock Concentration (mM)	Final concentration (mM)	Dissociation Factor	Osmolarity (mOsm)	Volume to add (uL)
dextran 6000	20	5	1	5	12.5
Glycerol	100%	15%	0	0	7.5
KCl	1000	135	2	270	6.8
MgCl2	1000	4.5	3	13.5	0.2
pLL	2.22	0.22	155	34.1	5.0
cy5pLL	0.16	0.01	1	0.01	3.1
TrisHCl	1000	22	1.84	40.48	1.1
alpha-hemolysin	0.015	0.0015		34.6	5
beta-galactosidase	1KU in 50% glycerol, 5 mM Tris Cl, 5 mM MgCl2, 0.5 mM DTT, 0.5 mM mercaptoethanol	10		2.52	5
H2O					3.8
Total				400.21	50

Outer aqueous	Stock Concentration (mM)	Final concentration (mM)	Dissociation Factor	Osmolarity (mOsm)	Volume to add (uL)
Glucose	1000	39.21	1	39.21	3.921
Glycerol	100%	15%	0	0	15
KCl	1000	150	2	300	15
MgCl2	1000	5	3	15	0.5
TrisHCl	1000	25	1.84	46	2.5
P188	10000	5000	0	0	50
H2O					13.079
Total				400.21	100

Exit hole solution	Stock Concentration (mM)	Final concentration (mM)	Dissocation Factor	Osmolarity (mOsm)	Volume to add (uL)
Glucose	1000	9.21	1	9.21	0.921
Glycerol	100%	15%	0	0	15
KCl	1000	150	2	300	15
MgCl2	1000	5	3	15	0.5
TrisHCl	1000	25	1.84	46	2.5
ATP	100	10	3	30	10
Fluorescein di-β-D-galactopyranoside (FDG)	10	0	1	1	0
H2O					56.079
Total				400.21	100

Glucose = osmotic compensator
use the low-binding tubing for the IA

EX14 06/07/2018 B-galactosidase pLL ADP

Inner aqueous	Stock Concentration (mM)	Final concentration (mM)	Dissociation Factor	Osmolarity (mOsm)	Volume to add (uL)
dextran 6000	20	5	1	5	12.5
Glycerol	100%	15%	0	0	7.5
KCl	1000	135	2	270	6.8
MgCl2	1000	4.5	3	13.5	0.2
pLL	2.22	0.22	155	34.1	5.0
cy5pLL	0.16	0.01	1	0.01	3.1
TrisHCl	1000	22	1.84	40.48	1.1
alpha-hemolysin	0.015	0.0015		34.6	5
beta-galactosidase	1KU in 50% glycerol, 5 mM Tris Cl, 5 mM MgCl2, 0.5 mM DTT, 0.5 mM mercaptoethanol	10		2.52	5
H2O					3.8
Total				400.21	50

Outer aqueous	Stock Concentration (mM)	Final concentration (mM)	Dissociation Factor	Osmolarity (mOsm)	Volume to add (uL)
Glucose	1000	39.21	1	39.21	3.921
Glycerol	100%	15%	0	0	15
KCl	1000	150	2	300	15
MgCl2	1000	5	3	15	0.5
TrisHCl	1000	25	1.84	46	2.5
P188	10000	5000	0	0	50
H2O					13.079
Total				400.21	100

Exit hole solution	Stock Concentration (mM)	Final concentration (mM)	Dissocation Factor	Osmolarity (mOsm)	Volume to add (uL)
Glucose	1000	19.21	1	19.21	1.921
Glycerol	100%	15%	0	0	15
KCl	1000	150	2	300	15
MgCl2	1000	5	3	15	0.5
TrisHCl	1000	25	1.84	46	2.5
ADP	100	10	2	20	10
Fluorescein di-β-D-galactopyranoside (FDG)	10	0	1	0	0
H2O					55.079
Total				400.21	100

Glucose = osmotic compensator
use the low-binding tubing for the IA

BIBLIOGRAPHY

[1] Libretexts, *Charged lipids,* (2017).

[2] R. Rand and V. Parsegian, *Hydration forces between phospholipid bilayers,* Biochimica et Biophysica Acta (BBA)-Reviews on Biomembranes **988**, 351 (1989).

[3] R. Phillips, J. Kondev, J. Theriot, H. G. Garcia, and N. Orme, *Physical biology of the cell* (Garland Science, 2013).

[4] P. Nelson, *Biological physics: energy, information, life ; with new art by David Goodsell* (Freeman, 2014).

[5] *phospholipid bilayers,* Brooklyn CUNY .

[6] V. J. Novak, *Present state of the coacervate-in-coacervate theory; origin and evolution of cell structure,* Origins of Life **14**, 513 (1984).

[7] *Liquid-liquid phase separation in biology,* The Annual Review of Cell and DevelopmentalBiology .

[8] A. Kudlay, A. V. Ermoshkin, and M. Olvera de La Cruz, *Complexation of oppositely charged polyelectrolytes: effect of ion pair formation,* Macromolecules **37**, 9231 (2004).

[9] D. Burgess, *Practical analysis of complex coacervate systems,* Journal of colloid and interface science **140**, 227 (1990).

[10] A. Veis, *A review of the early development of the thermodynamics of the complex coacervation phase separation,* Advances in colloid and interface science **167**, 2 (2011).

[11] A. Ye, *Complexation between milk proteins and polysaccharides via electrostatic interaction: principles and applications–a review,* International journal of food science & technology **43**, 406 (2008).

[12] C. P. Brangwynne, C. R. Eckmann, D. S. Courson, A. Rybarska, C. Hoege, J. Gharakhani, F. Jülicher, and A. A. Hyman, *Germline p granules are liquid droplets that localize by controlled dissolution/condensation,* Science **324**, 1729 (2009).

[13] C. P. Brangwynne, *Soft active aggregates: mechanics, dynamics and self-assembly of liquid-like intracellular protein bodies,* Soft Matter **7**, 3052 (2011).

[14] F. J. Anthony A. Hyman, Christoph A. Weber, *Phase behaviour and complex coacervation of aqueous polypeptide solutions,* (2012).

[15] S. Deshpande, Y. Caspi, A. E. Meijering, and C. Dekker, *Octanol-assisted liposome assembly on chip,* Nature communications **7**, 10447 (2016).

[16] S. Deshpande, F. Brandenburg, A. Lau, W. K. Spoelstra, S. S. W. Venkata, L. Reese, M. Dogterom, and C. Dekker, *Controlled formation of functional membrane-less organelles in liposomes,* in preparation (2018).